CHARACTERIZATION OF ERODIBLE SURFACES WITH AN ENVIRONMENTAL WIND TUNNEL

Dentoni V., Grosso B., Massacci G., Pinna F.

Dipartimento di Ingegneria Civile, Ambientale e Architettura,
Università degli Studi di Cagliari, Via Marengo 2, Cagliari, Italia

Abstract: *The article illustrates the design and the main characteristics of the Environmental Wind Tunnel (EWT) recently built in the laboratories of Cagliari University (DICAAR). The aim of the EWT is the simulation of a part-depth Atmospheric Boundary Layer (ABL) and thus the reproduction of the wind flow over any type of surface. Experimental tests are currently being performed to analyse the correlation between the emission of dust from a variety of erodible samples and the influencing physical parameters (moisture content, percentage of silt, particles density and wind speed). The final aim of the ongoing research is the definition of reliable Emission Factors (EFs) to represent the contribution of tailing basins, mine dumps and stockpiles to the overall emission of particulate matter (PM) from industrial sites and open yards exposed to wind erosion (industrial wind erosion).*

Keywords: dust emission; fugitive dust sources; industrial wind erosion, mine dumps, tailing basins, stockpiles.

1 Introduction

The emission of Particulate Matter (PM) from industrial sites derives from both conveyed and fugitive dust sources [1]. Typical examples of fugitive dust sources are working operations involving bulk material handling in open yards (loading, dumping and storing) and transportation along unpaved roads, as well as the wind action over the erodible surfaces of storage piles, mineral dumps and tailing basins (*industrial wind erosion*) [2].

While the emission flow from conveyed sources is relatively easy to estimate, the characterization of fugitive dust sources requires the knowledge of the specific working activity under exam (working cycle, duration of elementary phases, machinery characteristics, etc.), the physical properties of the emissive materials (humidity, silt content, density, grain size, etc.) and the specific anemological conditions of the geographic area. As regards *industrial wind erosion*, in particular, the emission of fine particles depends on the extent and orientation of the surfaces exposed to the wind action, the physical characteristics of the material composing those surfaces and the anemological conditions of the site. The variables that influence the erosion mechanism are numerous and of complex evaluation, so that general emission models only interpret the main laws governing the phenomenon, while the most complex and detailed aspects are taken into account by using site-specific parameters [3].

In order to determine the relationships between the emission flows and the specific characteristics of the erodible surfaces under investigation, a laboratory equipment has been designed and manufactured at DICAAR, in Cagliari University, which includes an open circuit

Environmental Wind Tunnel (EWT). The following paragraphs describe the DICAAR EWT and the experimental procedures currently being performed on erodible samples from a major tailing basins and from various industrial and mine sites.

2 Environmental wind tunnel studies

Laboratory tests aimed at investigating the emission of particulate matter (PM) from erodible surfaces by means of Environmental Wind Tunnels have been performed since 1941, when Bagnold studied the erosion of sandy surfaces and defined the correlation between the sand flow and the third power of the friction velocity [4]. The design of the DICAAR Wind Tunnel is based on an accurate review of consistent research studies carried out worldwide [5-11]. The literature review has been focused on open circuit suction type wind tunnels. In fact, open circuit tunnels are easier to design, require less space and lower construction costs. In addition, the power consumption for performing emission tests is minimal and the incremental capital cost for closing the circuit is not justified by the minor operating costs typical of closed-circuit wind tunnels [12-13]. In the suction type tunnel the fan is mounted at the end of the tunnel and pulls the air through the working section, so that the air entering the tunnel is undisturbed by the rotating fan and the negative pressure inside the tunnel keeps all removable doors and lids pressed against their intended positions [4].

Figure 1 shows the scheme of an open-circuit EWT [14], which is commonly composed of a Convergence section (CS), a Flow development section (FDS), a Test section (TS) and a final Drive section (DS).

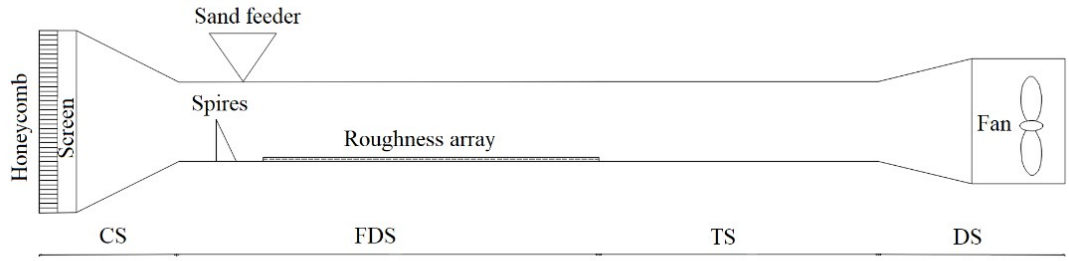

Figure 1. Schematic representation of an Environmental Wind Tunnel.

The *Convergence section* is meant to remove the disturbances from the ambient air and produce a uniform velocity profile. The contraction of the tunnel cross-section causes the acceleration and the alignment of the air entering the Flow development section and simultaneously reduces the turbulence [15-17]. A large contraction ratio is not essential when the turbulence reduction is not required or the experimental wind speeds are relatively low [13].

In order to reduce the ambient vortexes, a honeycomb flow-straightener is frequently mounted at the tunnel entrance, followed by one or more wire mesh screens. The honeycomb flow-straightener is a grid of small tubes with hexagonal cross-section, arranged coaxially to the

tunnel, which turn the flow parallel to the tunnel longitudinal axis and reduce the fluctuations along the vertical cross sections [16, 18]. The mesh screens are used to homogenize the velocity profile by reducing the longitudinal turbulence: the metal wires break larger eddies in a greater number of smaller vortices of the same size [12].

The *Flow development section* is required to generate the ABL before the Test Section, where the samples and the measurement instruments are placed. ABLs of different thickness can be reproduced by attaching to the floor of the Flow development section a combination of roughness arrays and spires. The surface roughness is simulated by means of basic geometric shapes, such as cubes or cylinders, or sandpaper sheets (in case of very low roughness). Spires consist of triangular flat plates facing the entering flow and equipped with a downwind splitter plate [19]; they are commonly used to accelerate the ABL rate of growth [12, 20]. When the effect of saltation needs to be taken into account, a sand feeder is also inserted at the entrance of the Flow development section to provide a flow of bouncing particles.

In the *Test section* the samples are placed along the floor in removable trays. The wind velocity and the dust concentration are measured in the Test section. The Flow development section and Test section define the tunnel Working section.

The tunnel final section is the *Drive section*, usually designed with divergent walls to induce flow deceleration and provide a continuous transition from a rectangular to a circular cross-section, which enables to install the fan at the tunnel end.

3 The DICAAR Wind Tunnel

The DICAAR Wind Tunnel depicted in Figure 2 includes a 1.5 m long *Convergence section*, a *Working section* (0,85 m high and 0.50 m wide), consisting of a *Flow development section* and a *Test section*, and finally a 2 m long Drive section, which houses a 5.5 kW axial fan.

A 1,50 m high and 0.80 m wide honeycomb flow straightener is placed at the tunnel entrance. The length to diameter ratio of the honeycomb cells is 8, enough to straighten the air flow and make it parallel to the tunnel longitudinal axis, according to the indications of Metha & Bradshaw [16] and Mathew et al. [18]. A wire mesh screen is inserted at the end of the CS to allow the reduction of the longitudinal turbulence.
The Flow development section length exceeds the minimum length suggested by White and Mounla [20], in order to develop the saltation's equilibrium state. At the entrance of the *FDS*, two triangular spires are attached to the tunnel floor to provide the acceleration of the ABL rate of growth. The spires characteristics were determined with reference to Irwin method [19]. In the 5 m long FDS, a real scale ABL is reproduced by means of sandpaper sheets with same surface roughness of the erodible samples to be tested. Sand particles are fed from a feeder mounted 0.25 m downstream of the FDS entrance.

In Test section a 50 cm long, 2 cm deep and 20 cm niche is provided to insert the aluminium tray containing the sample to be tested, so that the sample surface and the tunnel floor define a continuous horizontal plane. One side of the Test section is made of Plexiglas, the transparent panel can be side-opened to simplify the placement of the mud samples and the measurements instruments (dust monitor DustTrak and pitot tubes).

The tunnel final section (the Drive section) is designed with divergent walls to induce the flow deceleration and provide a continuous transition from the rectangular to the circular cross-section and thus enable the installation of the 5.5 kW axial ventilator. The picture in Figure 3 shows the tunnel from the final Drive Section.

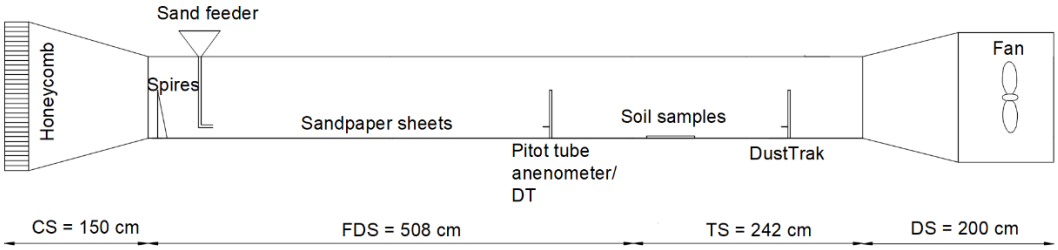

Figure 2. Schematic representation of the DICAAR EWT.

Figure 3. The DICAAR EWT.

3.1 Simulation of the required ABL

The simulation of the required ABL depends of two project parameters: δ (height of the boundary layer) and α (friction coefficient or Hellman exponent). The power-law wind profile (Equation 1), describes the mean vertical velocity profile to be reproduced before the tunnel test section:

$$u = u_\delta \left(\frac{z}{\delta}\right)^\alpha \quad (1)$$

where where u is the wind mean speed at a given distance z from the tunnel floor, u_δ is the wind speed at $z=\delta$ and α is the friction coefficient.

According to Irwin indications, two triangular spires combined with the consistent roughness (to be reproduced along the *Flow Development Section*) enables the simulation of the required ABL.

With specific reference to the red mud surfaces, two spires 0.53 m high and 0.035 m wide were designed and manufactured assuming δ=40 cm and α=0,10 as project parameters (Figure 4). Anemometric measurements were performed on site, at two different heights from the basin surface, to estimate the friction coefficient in the power-law wind profile (Equation 1) by means of Equation 2:

$$\alpha = \frac{\ln(u_1) - \ln(u_2)}{\ln(z_1) - \ln(z_2)} \quad (2)$$

where u_1 and u_2 are the wind mean speeds measured at z_1 (2 m) an z_2 (7 m). The arithmetic mean of the friction coefficient (0,10), corresponding to a surface roughness (z_0) of 0,2 mm, has been assumed as project parameter. In order to simulate the required field roughness, the FDS was coated with an 80 grit size abrasive paper. The value δ=40 cm was assigned to be about half the height of the Flow development section, according to the indications of Al Nehari et al. [17]. Figure 4 shows the Flow development section's entrance, with the two spires and the abrasive paper at the tunnel floor; both designed to reproduced the ABL over the red mud basin's surfaces.

Figure 4. Triangular spires installed at the entrance of the FDS.

3.2 Validation of the vertical wind profiles

A series of wind speed tests were performed in the tunnel Test section to verify the accuracy of the generated ABL. The measurements were performed for six different rotation velocity of the fan, along three vertical lines laying on the tunnel cross-section, just before the *Test Section* (before the sample to be tested). The mean values of the wind velocity measured along the three lines were found comparable, proving the transversal uniformity of the wind flow. The power-law wind profile described by Equation 1 was fitted to the experimental data, up to 40 cm from the tunnel floor. The results proved the DICAAR EWT to be capable of generating the required part-depth ABL, thus confirming the results obtained by Al Nehari et al. [17] and Lopes et al. [21]. The validation of the vertical wind profiles inside the tunnel is fully described in a previous article [14].

4 Experimental procedure

Emission tests are currently being performed on different samples of erodible materials from various industrial and mine sites within the Sardinian territory. Two types of PM sources are under consideration: stockpiles of bulk material (surfaces with finite erosion potential) and tailing basins (surface with infinite erosion potential).

According to the experimental procedure, for each aggregate material under investigation the following preliminary actions must be carried out before starting the emission tests:

1. Tunnel set up (choice of appropriate spires size and tunnel floor roughness);
2. Quantification of the sample moisture content (oven-drying method for 24 h at 105°C);
3. Sieve analysis and definition of the sample Particle Size Distribution (PSD);
4. Definition of the material mineralogical composition;
5. Quantification of the particles density.

As mentioned before, the tunnel set up must be defined with reference to the specific roughness of the erodible surface under investigation (step 1). The samples to be tested must be first dried for 24 h at 105°C (step 2) do determine the moisture content by differential weighting (before and after drying) and then rewetted to the desired water contents [7]. Alternatively, the humidity reduction curves can be defined as a function of the time spent in the oven at 105°C (Figure 5). The sieve analysis (step 3) is performed according to the US-EPA procedure for the experimental estimation of the threshold shear velocity [2].

Once the preliminary steps are performed, the aggregate material is placed in the sample tray and its surface is accurately levelled. The tray containing the sample to be tested is finally inserted inside the niche, in the tunnel's Test section, so that the sample surface and the tunnel floor define a continuous plan of constant roughness. The PM concentration is measured at different heights with a DustTraks 8533 DRX laser photometer installed 1 m downwind from the sample (Figure 6).

The fan operating regimes and the corresponding flow velocity at 40 cm from the tunnel floor are reported in Table 1. The graph in Figure 7 represents mean wind profile for the experimental speed range under consideration.

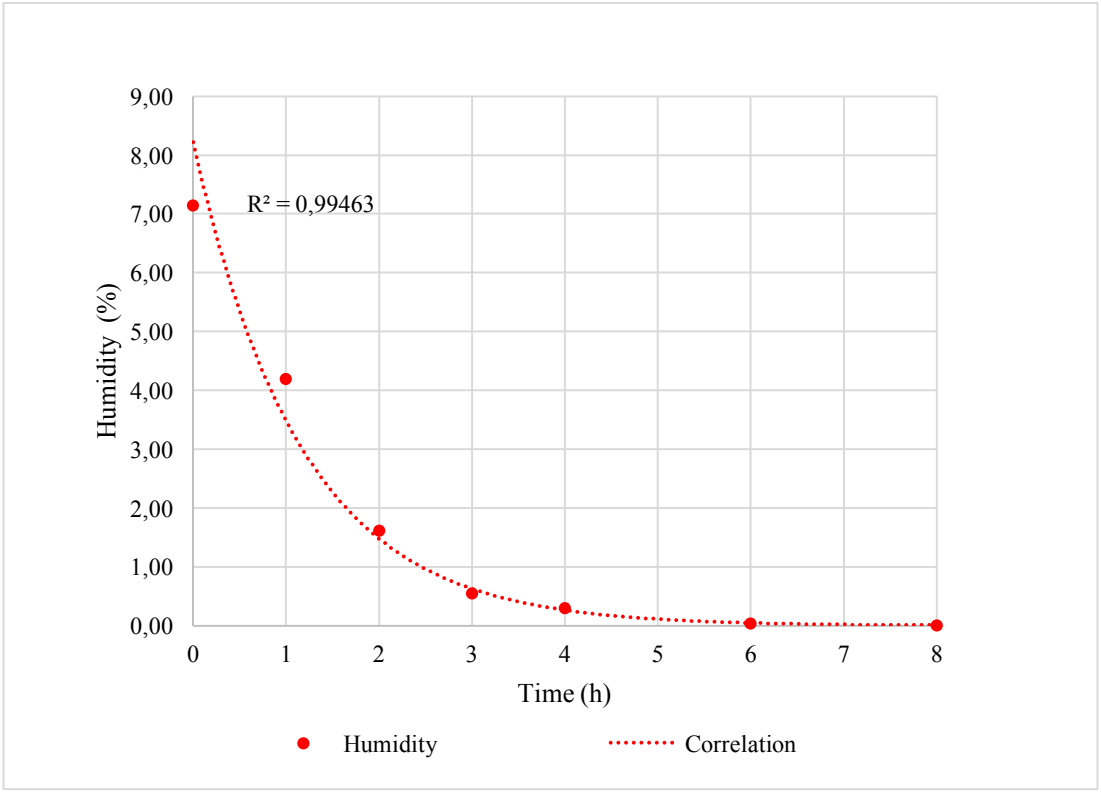

Figure 5. Humidity reduction curves vs time in the oven at 105°C.

(a) (b)

Figure 6. Sample tray inserted in the tunnel niche (a) and dust detector divice outside the tunnel (b).

Table 1: Fan operating regimes and the corresponding mean wind velocity at 40 cm.

Fan operating regimes (Hz)	Mean wind speed u_{δ} (m/s)
50	17,66
45	16,10
40	14,61
35	13,3
30	11,8
25	10,25
20	8,57
15	6,49

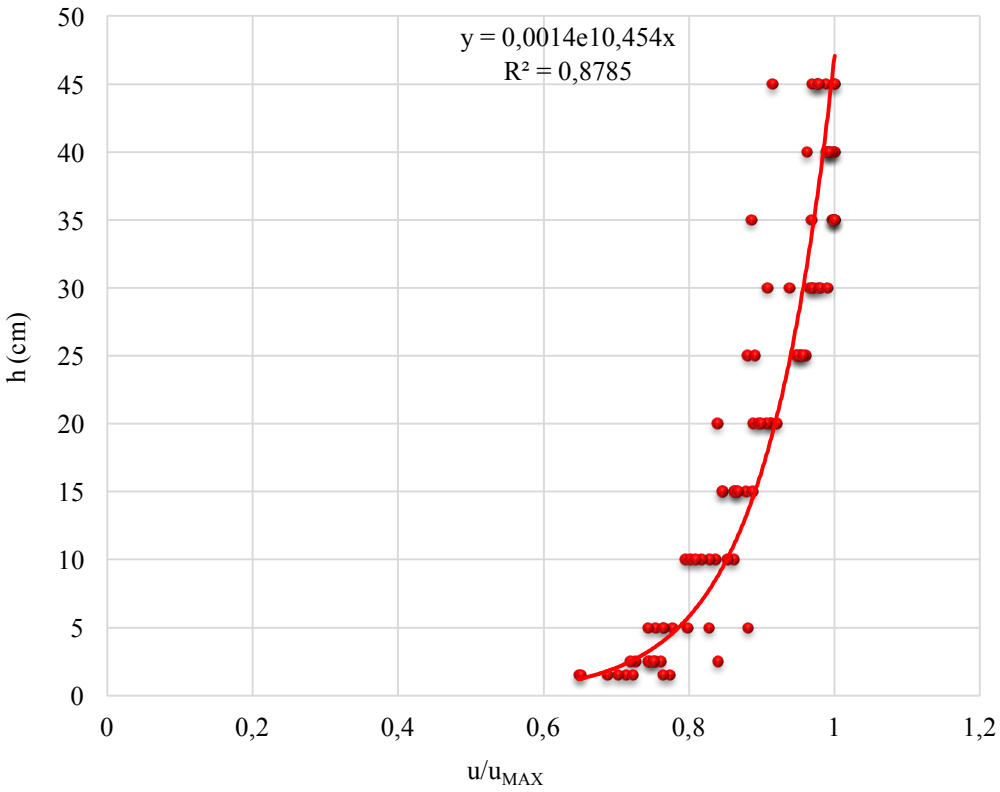

Figure 7. Mean wind profile for the experimental speed range.

For each material under investigation the emission test must be repeated at different heights, considering different values of the sample humidity and different fan velocities. Figure 8 represents a hypothetical representation of the experimental results for a single measurement point. The threshold velocities can be mathematically obtained for each experimental condition from the regression curves.

A further step will be the definition of the plume contour inside the tunnel and the measurement of the pairs *PM concentration-flow speed* in each point of a grid covering the plume cross-section. The pair values experimentally determined enable the calculation of the mass of dust emitted in the time unite and thus the Emission Factor (EF) of the tested sample in terms of mass emitted in the time and surface unite.

The erosion rates can be also calculated by weighing the sample before and after the test, in order to estimate the total mass of material removed from the sample surface.

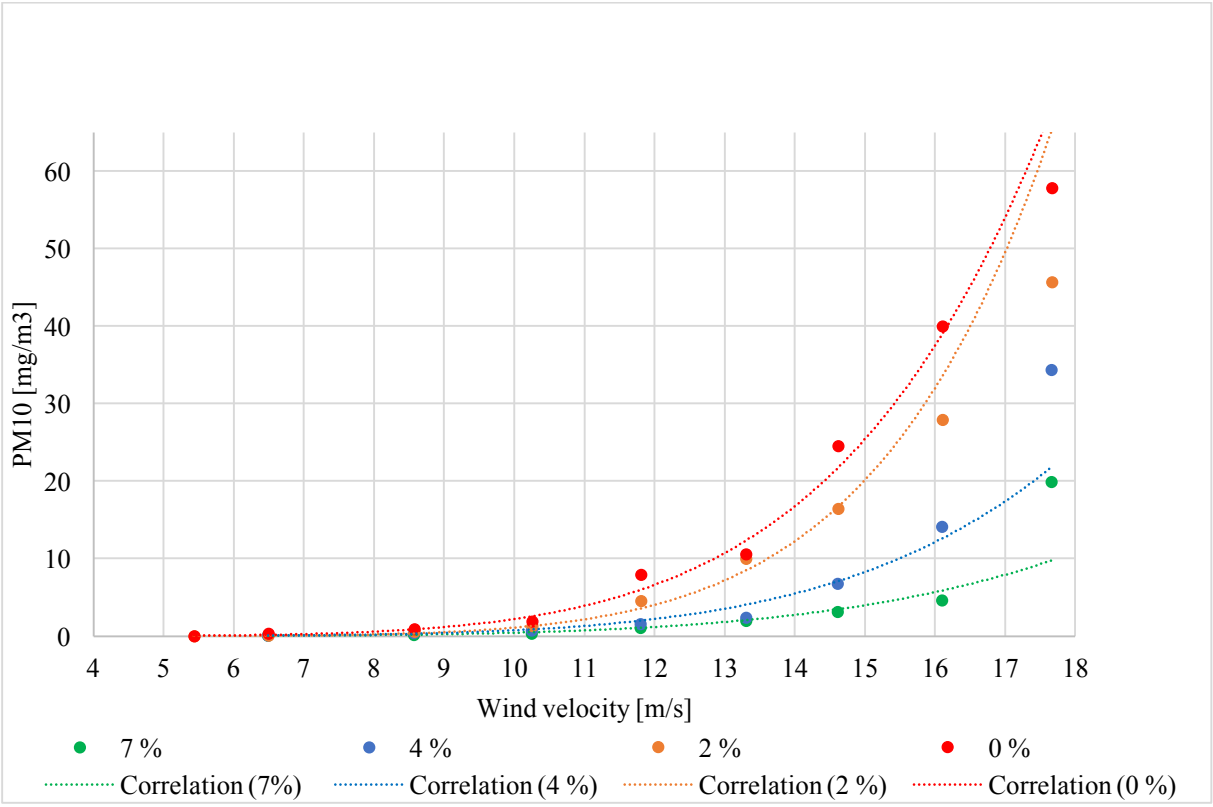

Figure 8. Correlation between PM10 concentration and wind speed different values moisture contents.

Conclusion

Environmental Impact Assessment (EIA) studies commonly implement air dispersion analysis to predict the atmospheric impact of conveyed and fugitive dust sources. The consistency of the impact prediction relies on the accuracy of the Emission Factors (EF) representing the dust sources under investigation.

Research studies are in progress in Cagliari University (DICAAR) to define site-specific Emission Factors (EFs) that could accurately represent the contribution of tailing basins, mine dumps and stockpiles to the overall PM emission from industrial sites and open yards exposed to wind erosion (industrial wind erosion).

The analysis of the erosion phenomenon requires the reproduction of the wind flow acting over the exposed erodible surfaces. To that aim, an Environmental Wind Tunnel (EWT) has been recently designed and built at DICAAR, which has proved to be capable of reproducing the required part-depth Atmospheric Boundary Layer (ABL).

Emission tests are currently being performed with the DICAAR EWT on a variety of samples from various industrial and mine sites located in Sardinia. Two types of PM sources are under consideration: stockpiles of bulk material and tailing basins.

For each sample of erodible material under investigation the humidity reduction curves are defined as a function of the drying process duration. For each value of the moisture content, the correlation between the PM10 concentration measured in the tunnel Test section and the wind velocity is analysed.

Further steps of the research include the calculation of Emission Factors (EF) for the types of material under exam, as well as the evaluation of the reduction measurements efficiency, with specific reference to the surfaces treatment with dust-binding substances.

Acknowledgement

Research carried out in the framework of projects conducted by CESA (Centre of excellence on environmental sustainability, Sardinia, Italy).

This work is part of the research project “RE-MINE - REstoration and remediation of abandoned MINE sites, funded by the Fondazione di Sardegna and Regional Sardinian Government (Grant CUP F72F16003160002).

Bibliography

1. Countess Environmental (2006). *WRAP Fugitive Dust Handbook*, final report for Western Governors’ Association 1515 Cleveland Place, Suite 200 Denver, Colorado 80202.
2. USEPA (2006) *Compilation of Air Pollution Emission Factors*, AP-42, Section 13.2.5 – Industrial wind erosion. United States Environmental Protection Agency.

3. Dentoni, V., Grosso, B., Massacci, G., Cigagna, M., Levanti, C., Corda, C. and Pinna, F. (2019) "Industrial wind erosion: PM emission from the erodible flat surfaces of tailing basins", 18th International Symposium on Environmental Issues and Waste Management in Energy and Mineral Production, Santiago, Chile, Springer, pp. 15–27. https://doi.org/10.1007/978-3-319-99903-6_2.
4. Bagnold, R.A. (1941) The Physics of Blown Sand and Desert Dunes, Menhuen, London. ISBN 978-94-009-5684-1.
5. Gillette, D. (1978) "A wind tunnel simulation of the erosion of soil: Effect of soil texture, sandblasting, wind speed, and soil consolidation on dust production.", Atmospheric Environ., Vol. 12 No. 12, pp. 1735-1743. https://doi.org/10.1016/0004-6981(78)90322-0.
6. Amante-Orozco, A. (2000) Fine Particulate Matter Generation under Controlled Laboratory and Wind Tunnel Conditions, PhD Dissertation, Texas Tech University, Lubbock, TX.
7. White, B.R. and Roney, J.A. (2000) Simulation and Analysis of Factors Leading to High PM10 Emissions Fluxes at Owens Dry Lake Using an Environmental Wind Tunnel, California Air Resources Board (CARB) Sacramento, California, University of California, Davis , CA.
8. Roney, J.A. and White, B.R. (2006) "Estimating fugitive dust emission rates using an environmental boundary layer wind tunnel", *Atmospheric Environment*, Vol. 40 No. 40, pp. 7668–7685.
9. McKenna Neuman, C., Boulton, J.W. and Sanderson, S. (2009) "Wind tunnel simulation of environmental controls on fugitive dust emissions from mine tailings", *Atmospheric Environment*, Vol. 43, pp. 520–529. https://doi.org/10.1016/j.atmosenv.2008.10.011.
10. Massey, J. (2013) *A Wind Tunnel Investigation to Examine the Role of Air Humidity in Controlling the Threshold Shear Velocity of a Surface and in Controlling the Mass Flux of Material from a Surface*, Master Thesis, Texas Tech University, Lubbock, TX.
11. Parajuli, S.P., Zobeck, T.M., Kocurek, G., Yang, Z.-L. and Stenchikov, G.L. (2016) "New insights into the wind-dust relationship in sandblasting and direct aerodynamic entrainment from wind tunnel experiments: DUST EMISSION STUDY USING A WIND TUNNEL", *Journal of Geophysical Research: Atmospheres*, Vol. 121 No. 4, pp. 1776–1792. https://doi.org/10.1111/j.1365-3091.2006.00775.x.
12. Van Dommelen, R. (2013) *Design of an Atmospheric Boundary Layer Wind Tunnel*, Master Thesis, Eindhoven University of Technology, Eindhoven.
13. Snyder, W.H. (1979) *The EPA Meteorological Wind Tunnel. Its Design, Construction, and Operating Characteristics*, U.S. EPA.
14. Dentoni V., Grosso B., Massacci G. and Pinna F. (2019) "Validation of a wind erosion model for tailings basins: Wind tunnel design and atmospheric boundary layer simulation", *International Journal of Mining, Reclamation and Enviroment*, https://doi.org/10.1080/17480930.2019.1678226 (in print).
15. Mehta, R.D. (1979) "The aerodynamic design of blower tunnels with wide-angle diffusers", *Progress in Aerospace Sciences*, Vol. 18, pp. 59–120. https://doi.org/10.1016/0376-0421(77)90003-3.
16. D. Mehta, R. and Bradshaw, P. (1979) "Design rules for small low speed wind tunnels. Aeronaut J Aeronaut Soc", *Aeronautical Journal -New Series-*, Vol. 83, pp. 443–449.
17. Al-Nehari, H.A., Abdel-Rahman, A.K. and El-Moneim, A. (2010) "Design and construction of a wind tunnel for environmental flow studies", p. 17.

18. Mathew, J., Bahr, C., Carroll, B., Sheplak, M. and Cattafesta, L. (2005) "Design, Fabrication, and Characterization of an Anechoic Wind Tunnel Facility", *11th AIAA/CEAS Aeroacoustics Conference*, presented at the 11th AIAA/CEAS Aeroacoustics Conference, American Institute of Aeronautics and Astronautics, Monterey, California. https://doi.org/10.2514/6.2005-3052.
19. Irwin, H.P.A.H. (1981), "The design of spires for wind simulation", *Journal of Wind Engineering and Industrial Aerodynamics*, Vol. 7 No. 3, pp. 361–366. https://doi.org/10.1016/0167-6105(81)90058-1.
20. White, B.R. and Mounla, H. (1991) "An experimental study of Froude number effect on wind-tunnel saltation", *Aeolian Grain Transport 1*, Springer, Vienna, pp. 145–157. https://doi.org/10.1007/978-3-7091-6706-9_9.
21. Lopes, M.F.P., Gomes, M.G. and Ferreira, J.G. (2008) "Simulation of the atmospheric boundary layer for model testing in a short wind tunnel*", Exp Tech*, 32, pp. 36–43.